THE JOURNAL OF PHYSICAL CHEMISTRY C

C: Surfaces, Interfaces, Porous Materials, and Catalysis

Reverse Hierarchy of Alkane Adsorption in Metal-Organic Frameworks (MOFs) Revealed by Immersion Calorimetry

Carlos Cuadrado-Collados, Cintia Karina Rojas-Mayorga, Beatriz Saavedra, Manuel Martínez-Escandell, Jacek M. Osinski, Peyman Z. Moghadam, David Fairen-Jimenez, and Joaquin Silvestre-Albero

J. Phys. Chem. C, **Just Accepted Manuscript** • DOI: 10.1021/acs.jpcc.9b01381 • Publication Date (Web): 10 Apr 2019

ACS Publications

is published by the American Chemical Society. 1155 Sixteenth Street N.W., Washington, DC 20036

Reverse Hierarchy of Alkane Adsorption in Metal-Organic Frameworks (MOFs) Revealed by Immersion Calorimetry

Carlos Cuadrado-Collados,[1] Cintia K. Rojas-Mayorga,[1] Beatriz Saavedra,[1] Manuel Martinez-Escandell,[1] Jacek M. Osiński,[2] Peyman Z. Moghadam,[3] David Fairen-Jimenez,[2] Joaquin Silvestre-Albero[1,]*

[1]Laboratorio de Materiales Avanzados, Departamento de Química Inorgánica-Instituto Universitario de Materiales, Universidad de Alicante, E-03690 San Vicente del Raspeig, Spain [2]Adsorption & Advanced Materials Laboratory (AAML), Department of Chemical Engineering & Biotechnology, University of Cambridge, Philippa Fawcett Drive, Cambridge CB3 0AS, UK [3]Depatment of Chemical and Biological Engineering, University of Sheffield, Mappin Street, Sheffield S1 3JD, UK

ABSTRACT

Immersion calorimetry into liquids of different dimensions is a powerful tool to learn about the pore size and shape in nanoporous solids. In general, in the absence of specific interactions with the solid surface, the accessibility of the liquid probe molecule to the inner porosity, and the associated enthalpy value decreases with an increase in its kinetic diameter (bulkier molecules have lower accessibility and packing density). Although this is true for majority of solids (e.g. activated carbons and zeolites), this study anticipates that this is not straightforward in the specific case of MOFs. The evaluation of different hydrocarbons and their derivatives reveals the presence of reverse selectivity for C_6 isomers (2,2-dimethylbutane>2-methylpentane>n-hexane) in UiO-66 and HKUST-1, while size exclusion effects take place in ZIF-8. The immersion calorimetric findings have been compared with vapor adsorption isotherms and computational studies. Monte Carlo simulations suggest that the reverse selectivity in UiO-66 are attributed to the strong confinement of the di-branched hydrocarbons in the small tetragonal cages, while the presence of strong interactions with the open metal sites account for the preferential adsorption in HKUST-1. These results open the gate towards the application of immersion calorimetry for the pre-

screening of MOFs to identify in an easy, fast and reliable way interesting characteristics and/or properties such as separation ability, reversed hierarchy, pore-window size, presence of unsaturated metal sites, molecular accessibility, and so on.

1. INTRODUCTION

The separation of C_5 and C_6 isomers in the petrochemical industry is a crucial process for multiple applications, such as the increase of the octane number of the gasoline. For example, the octane number for n-hexane (n-hx), 2-methylpentane (2-MP) and 2,2-dimethylbutane (2,2-DMB) varies largely due to their linear or branched characteristics, with values that range between 24.8 and 91.8. In a typical isomerization reactor, the product stream contains a mixture of linear, mono- and di-branched isomers that must be separated and for what preferential adsorption of the higher octane number isomer is desired, so that the non-isomerized products can be recycled back to the isomerization unit.[1] Traditionally, isomers separation in conventional adsorbents such as activated carbons, zeolites and clays with narrow porous networks follow the natural order of size and shape selectivity, i.e. the linear hydrocarbons are preferentially adsorbed due to their smaller kinetic diameter, while bulkier ones are partially or totally excluded.[2-4] However, some specific zeolites (e.g., MCM-22, CFI and MFI) also show the so-called *inverse alkane adsorption hierarchy*, where branched hydrocarbons are preferentially adsorbed versus their linear analogues.[1,5-7] In this context, the development of novel porous materials capable of retaining isomerized

compounds would allow to improve the process significantly, improving efficiency and reducing the final cost.

Metal-organic frameworks (MOFs) are one of the most widely investigated porous materials nowadays due to their exceptional performance in a wide range of industrial applications, including gas storage and separation processes, catalytic applications, and sensors.[8-11] With more than 88,000 structures in the Cambridge Structural Database (CSD), the excellent performance of MOFs lies in the diverse potential combinations of metallic clusters/centers, and bridging organic ligands, which provides an almost infinite number of structures with diverse physical and chemical properties that can be tuned to, in principle, any application.[10-13] The high performance of MOFs is usually based on a highly developed porous structure, such as large accessible surface area and large pore volumes, and tunable surface chemistry. However, this large combination of possibilities bring challenges regarding the understanding and prediction of their adsorption behavior.

To help the understanding of the adsorption phenomena in MOFs, numerous research has been reported combining advanced experimental techniques and molecular simulations. Related to the adsorption of branched alkanes, Dubbeldam et al. used configurational-bias Monte Carlo simulations on a large variety of

nanoporous adsorbents, showing the potential of MOFs to exhibit the "abnormal" inverse hierarchy.[14] These theoretical predictions have been experimentally confirmed for UiO-66 using breakthrough column experiments.[15] Bárcia et al. attributed the preferential adsorption of bulky hydrocarbons versus the linear counterparts on UiO-66 to the free rotation of the branched molecules — the rotational entropy effect — inside the small tetrahedral cavities, results that were further confirmed by Ramsahye et al. using chromatographic experiments.[15,16] Despite the technological importance of this phenomenon, the number of experimental studies dealing with inverse selectivity is scarce, whereas the adsorption phenomena at the molecular level is difficult to understand.

To tackle this challenge, we propose the use of immersion calorimetry combined with vapor adsorption and molecular simulations. Immersion calorimetry is a powerful technique for the characterization of the porous texture and surface chemistry of nanoporous solids. In the absence of specific interactions at the solid-liquid interphase, the enthalpy of immersion of a certain molecule into a solid is proportional to its accessible surface area.[3] In other words, the technique allows analyzing the pore size distribution of a porous solid by using probe molecules with different kinetic diameters. Although this is straightforward for activated carbons, zeolites, and ordered mesoporous silica, herein

we show that this is not the case for MOFs. To our knowledge, this is the first time that this technique has been applied in a deep evaluation of MOFs and in this critical industrial application. We evaluate the potential of immersion calorimetry for MOFs, not only to provide information about the size and shape of the porosity, but also to identify the adsorption properties of MOFs, including the reverse hierarchy adsorption behavior.

2. EXPERIMENTAL SECTION

2.1. Sample preparation and characterization

For this study three different MOFs have been selected: ZIF-8, HKUST-1 and UiO-66. The first two MOFs were commercially available from Sigma-Aldrich (Basolite Z1200 and Basolite C300, respectively), while UiO-66 was synthesized following the following receipt: 0.125 g of $ZrCl_4.H_2O$ was dissolved in 5mL DMF and 1 mL HCl (37%). 0.125 g of terephthalic acid was dissolved in 10 mL DMF. The two solution was mixed and left in an oven at 353 K for 16 hours. After centrifugation, the collected solid was washed by DMF (3x15 mL) and ethanol (3x30 mL) before drying in an incubator at 353 K.

The quality of the MOFs was evaluated by X-ray diffraction and gas adsorption measurements at cryogenic temperatures (N_2 and Ar at 77 K). XRD measurements were performed in a Bruker D8-Advance with

mirror Goebel and an X-ray generator KRISTALLOFLEX K 760-80F (power: 3000W, voltage: 20-60 KV and current: 5-80 mA) using a copper anode. Gas adsorption measurements were performed in a home-made high-resolution manometric equipment, now commercialized by G2Materials (http://www.g2mtech.com). Before the adsorption measurements the samples were degassed at 383 K for 12 h.

Immersion calorimetry measurements were performed in a SETARAM C80D calorimeter working at 303 K. A more detailed explanation of the experimental set-up can be found elsewhere.[3] For each MOF-liquid probe molecule pair, immersion enthalpy measurements were repeated 2-3 times, the standard deviation obtained being < 5% in all cases. Vapour adsorption isotherms were performed at 298 K in a homemade manometric equipment, now commercialized by Quantachrome Corp. as VSTAR equipment. Before the calorimetric measurements and the vapour adsorption experiments, samples were degassed under ultra-high vacuum conditions at 383 K for 12h.

2.2. Computational Methods

C_6 isomers adsorption in ZIF-8, HKUST-1 and UiO-66 was investigated using configurational bias grand canonical Monte Carlo (CB-GCMC) simulations implemented in the multipurpose simulation code RASPA.[17] In the grand canonical ensemble, the chemical potential, the volume and the temperature are kept fixed to mimic adsorption experiments. The chemical potential is related to the system

pressure by the Peng-Robinson equation of state. In the simulation, molecules are randomly moved, grown, inserted and deleted allowing the number of molecules in the framework to fluctuate.

An atomistic model was used for the MOFs, where the framework atoms were kept fixed at the crystallographic positions (details can be found in Tables S1-S3). The standard 12-6 Lennard-Jones (LJ) potential was used to model the dispersive interatomic interactions. The parameters for the framework atoms were obtained from the DREIDING force field (DFF)[18] where available and the Universal Force Field (UFF)[19] otherwise. All C_6 isomers were modelled using the united atom TraPPE potential.[20] The Lorentz-Berthelot mixing rules were employed to calculate adsorbate-framework and adsorbate-adsorbate parameters. Interactions beyond 12.8 Å were neglected in the simulations.

3. RESULTS AND DISCUSSION

Powder X-ray diffraction (PXRD) analyses of the porous materials were performed to evaluate the purity of the crystalline phases in ZIF-8, HKUST-1 and UiO-66. Figure S1 shows the PXRD patterns for the three materials evaluated. As it can be appreciated, there is a perfect agreement between the experimental and the simulated patterns. This observation confirms the quality of the evaluated MOFs and rules out the formation or presence of secondary phases.

Besides the crystallographic fingerprint, one of the most important parameters defining the quality of a given nanoporous material is its textural properties, i.e. the knowledge of the framework and channels network. Among the different possibilities for the textural characterization of MOFs, N_2 and Ar adsorption at cryogenic temperatures have been proposed in the literature as the most recommend probe molecules for the characterization of this kind of solids.[21] Although N_2 adsorption at cryogenic temperatures has been the most widely applied method, nitrogen is a diatomic molecule with a quadrupole moment and it can give rise to uncertainties when dealing with samples with small micropores or a rich surface chemistry.[22] On the contrary, Ar is spherical and it does not possess a quadrupole moment. The lack of quadrupole moment for Ar is very important because it avoids the presence of specific interactions with most surface functional groups and exposed ions, thus providing a more accurate description of the narrow micropore region. Figure S2 shows the N_2 and Ar adsorption/desorption isotherms at 77 K for the three MOFs evaluated in logarithmic scale. In general, the adsorption/desorption profiles for N_2 and Ar for each specific MOF are rather different, thus reflecting a different nature of the probe molecule-framework interactions depending of its physicochemical properties. As it can be observed in Table 1, there is a good agreement between the textural parameters obtained with

both probe molecules, mainly in the micropore and total pore volume, while larger differences area encountered in the BET are (effective cross-sectional area for nitrogen considered is 0.162 nm^2 and 0.138 nm^2 for argon). In any case, the obtained parameters are in perfect agreement with previous results described in the literature for these MOFs. A detailed description of the gas adsorption measurements can be found in the Supporting Information.

Table 1. MOF textural properties derived from the N_2 and Ar adsorption data at 77 K. Micropore volume (V_0) is estimated from the Dubinin-Radushkevich equation and total pore volume is estimated at $p/p_0 \cong 0.9$.

	N_2 adsorption data at 77 K			Ar adsorption data at 77 K		
Sample	S_{BET} (m^2/g)	V_0 (cm^3/g)	V_t (cm^3/g)	S_{BET} (m^2/g)	V_0 (cm^3/g)	V_t (cm^3/g)
ZIF-8	1674	0.62	0.67	1260	0.63	0.68
HKUST-1	1766	0.64	0.73	1740	0.65	0.67
UiO-66	1400	0.57	0.72	1590	0.62	0.65

To our knowledge the number of studies reported in the literature dealing with immersion calorimetry applied to MOFs is rather scarce.[23,24] To begin the calorimetry experiments, we first focused on measuring the enthalpy of immersion for a range of hydrocarbons

in the three MOFs. Figure 1 compares the enthalpy values, in a MOF weight basis, for dichloromethane (DCM – kinetic diameter = 0.33 nm), n-hexane (n-hx – kinetic diameter = 0.43 nm), 2-methyl-pentane (2-MP – kinetic diameter = 0.5 nm), 2,2-dimethyl-butane (2,2-DMB – kinetic diameter = 0.62 nm), alpha-pinene (kinetic diameter = 0.7 nm) and 1,3,5-triisopropylbenzene (1,3,5-TIPB – kinetic diameter = 0.85 nm). ZIF-8 exhibits a similar behavior than that of activated carbons and zeolites, with $-\Delta H_{imm}$ decreasing with an increase in the kinetic diameter of the probe molecule. Indeed, DCM exhibits the largest degree of interaction with an enthalpy value close to 90 J/g. ZIF-8 possess a sodalite (SOD) topology containing relatively large pore cavity of *ca.* 1.16 nm interconnected by small windows of *ca.* 0.34 nm (6 MR windows) and *ca.* 0.08 nm (4 MR windows).[25] Despite the predicted small window for ZIF-8, it is widely accepted that ZIF-8 is able to adsorb larger molecules, including butane with a kinetic diameter of 0.43 nm, due to the swinging of the methylimidazole (mIm) linker.[26] Immersion calorimetry into molecules above 0.4 nm clearly confirms this assumption. For instance, n-hexane with a kinetic diameter of 0.43 nm and 2-methylpentane with 0.50 nm are somehow able to access partially the inner porosity in ZIF-8 (enthalpy values 65 and 25 J/g, respectively). The partial accessibility of these two molecules to the inner cavities in ZIF-8 could be associated with a different swinging of the mIm linkers depending on the nature of

the hydrocarbons or to their lower packing density inside the cavities. However, MCGC simulations described later on rule out the last assumption. Larger molecules such as 2,2-dimethylbutane (2,2-DMB) with 0.62 nm are completely excluded from the inner porosity. Consequently, these calorimetric measurements clearly show that window size in ZIF-8 can flex and open up to *ca.* 0.5 nm, i.e. slightly above the simulated window size, the heat of immersion decreasing with the molecular size. This normal size and shape selectivity trend is in close agreement with the results obtained using activated carbons and zeolites.[3] However, the expected tendency observed in the majority of nanoporous materials is not straightforward in the case of some MOFs, as described below for HKUST-1 and UiO-66. At this point, it is important to highlight that the total enthalpy values obtained for ZIF-8 must be somehow underestimated due to the associated energy penalty required to swing the methylimidazolate linkers upon adsorption. In fact, Hobday et al. reported an energy value of 6.2 kJ/mol per mIm linker (*ca.* 27 J/g), for the rotation of the linker θ (angle between planes of the mIm atoms and the (100) crystallographic plane) from 65.1° to 87.8°.[27]

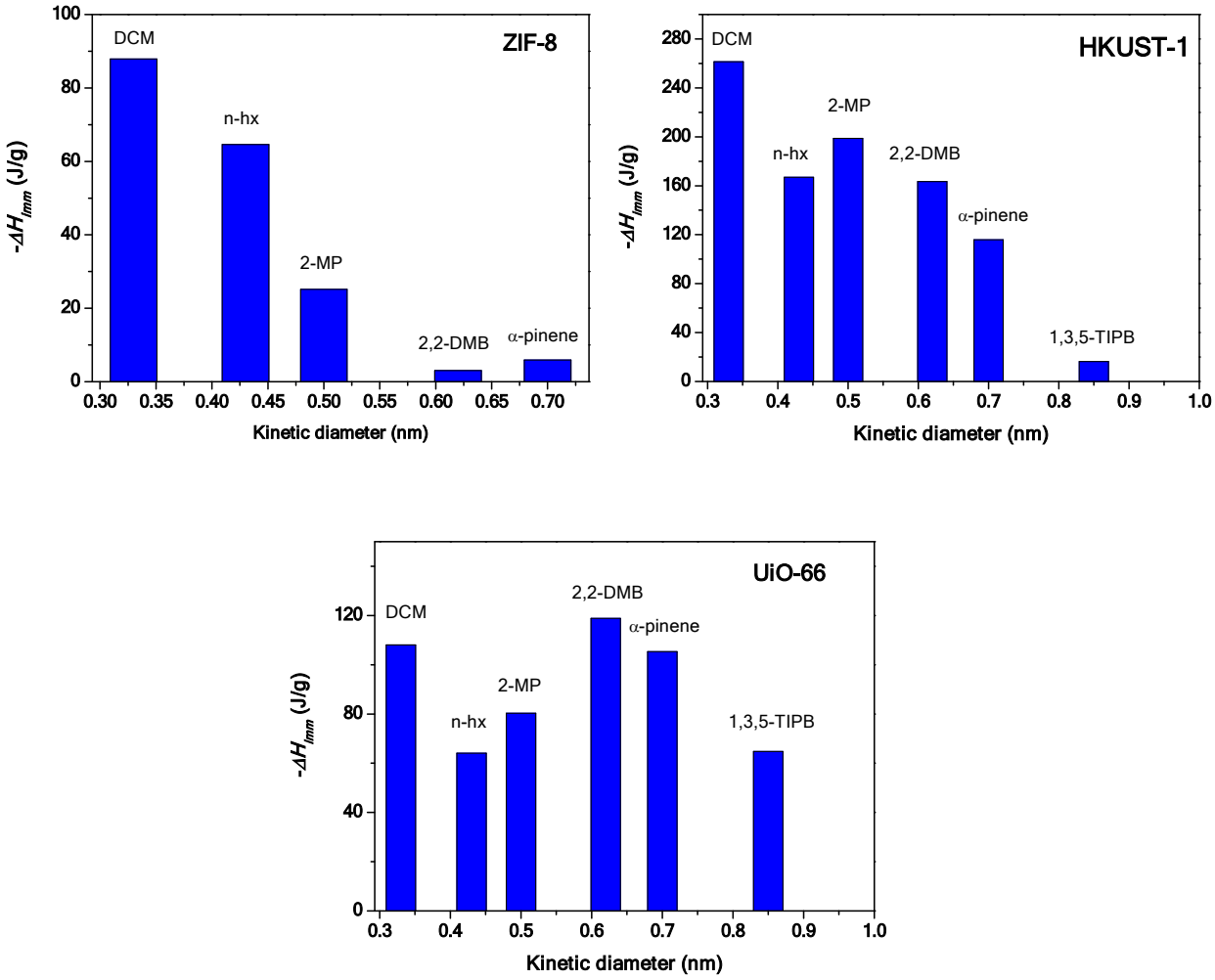

Figure 1. Enthalpy of immersion (J/g) for dichloromethane (DCM), n-hexane (n-hx), 2-methylpentane (2-MP), 2,2-dimethylbutane (2,2-DMB), alpha-pinene (α-pinene) and 1,3,5-triisopropylbenzene (1,3,5-TIPB) in ZIF-8, HKUST-1 and UiO-66.

HKUST-1 exhibits larger enthalpy values for all the molecules evaluated compared to ZIF-8 and UiO-66. For instance, DCM exhibits a total enthalpy of 260 J/g of HKUST-1, this value being close to

3 times larger than those obtained in UiO-66 and ZIF-8, as well as other nanoporous solids such as activated carbons and zeolites.[3] This observation clearly points to the presence of specific interactions between the evaluated molecules and the accessible acid Lewis centers in HKUST-1. Concerning the linear, mono- and di-branched C_6 isomers the order of enthalpy values does not follow the expected trend, i.e. the enthalpy increases from n-hx (167 J/g) to 2-MP (192 J/g), but then it decreases for 2,2-DMB (174 J/g). Alpha-pinene, a molecule with a kinetic diameter of 0.7 nm is also able to partially access the inner porosity (115 J/g), while 1,3,5-TIPB (kinetic diameter = 0.85 nm) is completely excluded. These results confirm that the maximum window size determined experimentally for HKUST-1 is around 0.7-0.85 nm, in close agreement with the simulated structure where the large cages in HKUST-1 (1.32 and 1.11 nm in diameter) are connected by 0.9 nm windows of square cross section.[28] Furthermore, the large cages are also connected to tetrahedral shaped side pockets of roughly 0.6 nm through triangular shaped windows of about 0.46 nm (0.35 nm in the hydrated form), thus explaining the larger enthalpy and accessibility for DCM as compared to the other hydrocarbons.

A similar reversed hierarchy performance is observed for UiO-66. In this MOF, the enthalpy of immersion decreases from DCM (108 J/g) to n-hx (64 J/g), as expected for a larger molecule. However,

the enthalpy rises up to a maximum of 120 J/g for 2,2-DMB, the enthalpy decreasing thereafter. Surprisingly, in UiO-66, even a large molecule such as 1,3,5-TIPB is able to access partially the porosity (enthalpy = 64 J/g), indicating that the maximum window size must be above 0.85 nm. This observation anticipates an underestimation in the simulated pore size window for UiO-66, since crystallographic predictions identify two different cavities, the large octahedral pores with 1.1 nm diameter and the small tetrahedral pores with 0.8 nm, the cavities being accessed through windows of 0.7 nm.[29] Table S4 summarizes the calorimetric data in gravimetric basis, i.e., per gram of MOF sample (J/g).

In summary, immersion calorimetry measurements into liquids of different molecular dimensions are able to anticipate, in a very simple, fast (a complete experiment takes ~ 1-2h) and reproducible way, three very important features defining the structure and performance of MOFs, i.e., i) the experimental pore-window size, ii) the presence of specific interactions between the probe molecule and the framework structure (e.g., due to unsaturated metal sites), and iii) the presence of normal or inverse size/shape selectivity.

In order to corroborate the liquid phase calorimetric observations, we also measured vapour adsorption isotherms for n-hex, 2-MP and 2,2-DMB in all three MOFs at 298 K. Figure 2 shows

the adsorption/desorption isotherms in linear and logarithmic scale for the different hydrocarbons evaluated up to $p/p_0 \approx 1$.

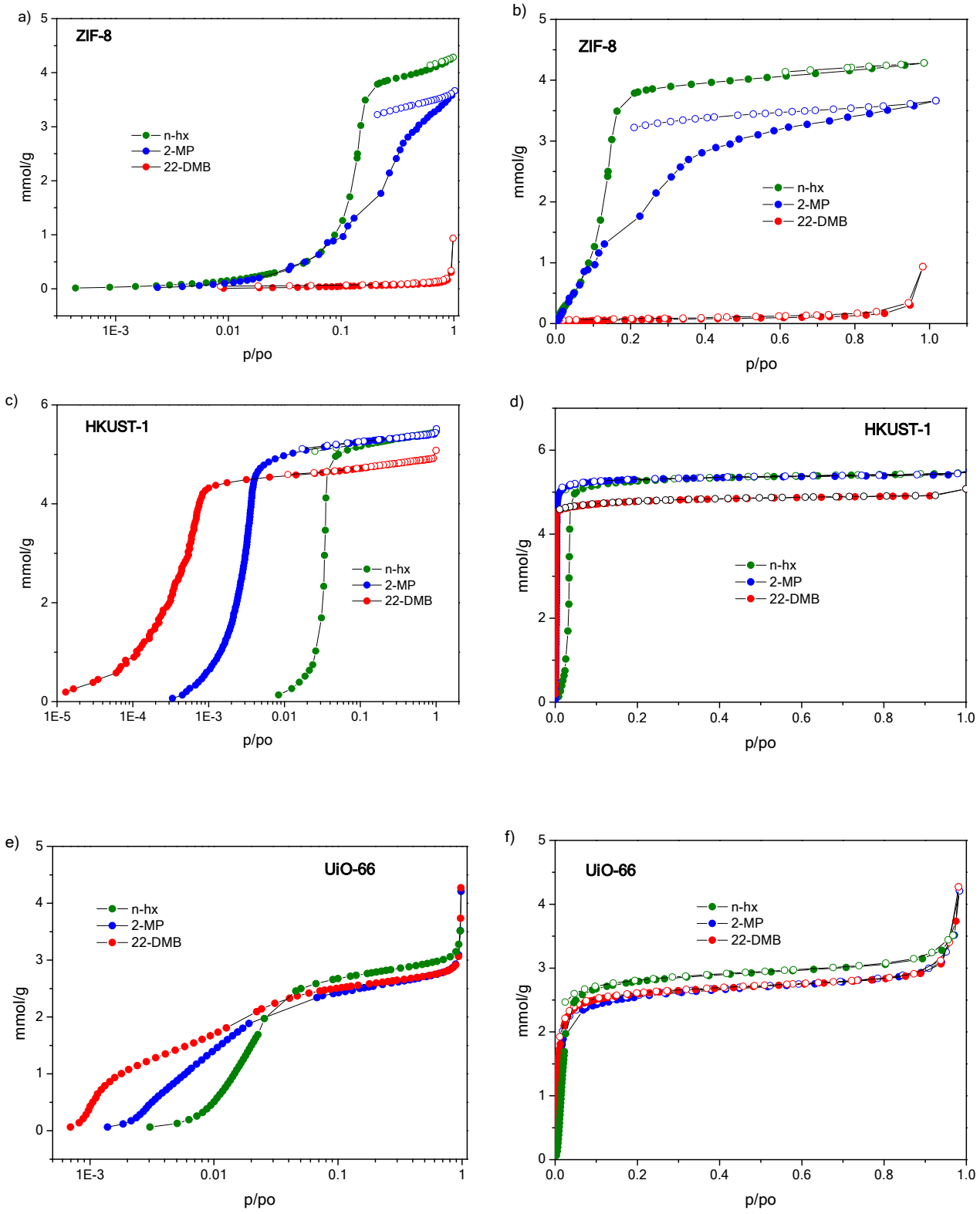

Figure 2. Vapour adsorption/desorption isotherms for ZIF-8, HKUST-1 and UiO-66 at 298 K in logarithmic (left column) and linear (right column) scales.

For ZIF-8, n-hex exhibits an S-shape isotherm with saturation uptake close to 4.3 mmol/g. The larger 2-MP is also able to access the porosity in ZIF-8 although with a smaller adsorption capacity (*ca.* 3.6 mmol/g). At low pressure regimes up to 0.1, both molecules start filling the cavities following a similar profile, thus suggesting the absence of specific interactions between the hydrocarbon and the solid framework. At this point it is important to highlight that the vapour adsorption isotherm for 2-MP took more than 2 weeks to reach equilibrium, pointing to the presence of serious kinetic limitations, in close agreement with the narrow ca. 0.5 nm pore window size identified with immersion calorimetry. The diffusional problems for 2-MP can be clearly reflected in the desorption branch, with a very small desorption even at very low relative pressures. Finally, 2,2-DMB does not adsorb over the entire pressure range. These results are in excellent agreement with the calorimetric data. Despite being a very simple, fast and easy experiment, immersion calorimetry was able to anticipate the full accessibility to the inner porous network for n-hx, the

partial accessibility for 2-MP and the complete exclusion for 2,2-DMB. To shed more light on the adsorption of hexane isomers in ZIF-8's flexible pores, two sets of GCMC simulations were carried out for ZIF-8 (Figure S3-S5). In the first set (Figure S3), the imidazolate linkers acting as windows to the cavities were kept open (corresponding to the high-pressure structure), while in the second one (Figure S4) they were kept closed (low-pressure structure). For both systems, the order of adsorption is predicted to be similar to the experiments with hexane adsorbed preferentially at lower pressures, especially in the closed ZIF-8 model. In contrast to experiments, the simulations predicted non-zero 2,2-DMB adsorption which stems from the fact that GCMC simulations do not take into account the accessibility of the windows connecting ZIF-8 large cavities –molecules are inserted at random positions– while in reality they would have to first pass through the narrow windows. The simulated saturation loading for all isomers is around 3.0 mmol/g, which is slightly smaller than those measured experimentally.

In HKUST-1, the adsorption isotherms show important differences depending on the hydrocarbon evaluated (Figure 2c-d). 2,2-DMB is the first molecule to fill the pores at 10^{-5} p/p_0, followed by 2-MP at 10^{-3} p/p_0 and n-hx at 10^{-2} p/p_0. This order of vapor adsorption clearly suggests the presence of reversed hierarchy in HKUST-1,

and further corroborates the results obtained from the immersion calorimetry, see Figure 1. However, we note the presence of certain differences between the two measurements. Among all the C_6 molecules, the calorimetry experiments provided a larger enthalpy value for 2-MP (192 J/g) compared to 2,2-DMB (174 J/g) and n-hx (167 J/g), whereas vapour adsorption measurements show stronger solid - 2,2-DMB interactions since it adsorbs first at the Henry regime, i.e. low pressures. At saturation loading, the order of adsorption changes: the total amount adsorbed for 2-MP and n-hx exhibits higher adsorption capacity (5.4 mmol/g) compared to 2,2-DMB with a total uptake of 4.9 mmol/g. This indicates that the enthalpy of immersion we measured in the liquid phase will not only depend on the adsorbate-framework interactions at low coverage but also in the number of molecules filling the inner cavities and the external surface. Indeed, the enthalpy of immersion corresponds to the heat generated when the solid surface is put in contact with a liquid wetting the whole surface. To further probe this phenomena, the enthalpy of immersion per gram of MOF (J/g) was converted into a "normalized" molar enthalpy of immersion (kJ/mol), i.e. enthalpy of immersion per mol of adsorbed hydrocarbon (Table 2). Although this is only an approximation because each technique evaluates a different state (liquid versus vapour), it can be useful to estimate the interaction of any single molecule filling the cavities (considering that the number of

molecules wetting the external surface is minimal compared to those wetting the inner porosity). The molar enthalpy is indeed similar for 2,2-DMB and 2-MP (*ca.* 35 kJ/mol), while the value for n-hx is smaller (*ca.* 31 kJ/mol). We note that although our calculations are merely an approximation because we cannot isolate the interactions between adsorbates filling the cavities and those wetting the surface in the calorimetry experiments, the normalized molar enthalpy values are in close agreement with those described in the literature for HKUST-1 at low coverage for n- and i-butane (isosteric heat of adsorption estimated experimentally *ca.* 32-35 kJ/mol), but far away from the GCMC predictions (*ca.* 60-80 kJ/mol for C_6 isomers in UiO-66 and HKUST-1). [16,30]

Table 2. "Normalized" molar enthalpy of immersion for the different MOFs evaluated (kJ per mol of adsorbed hydrocarbon) estimated from the immersion calorimetry measurements and considering the total amount adsorbed in the vapor adsorption experiments. Ratio of the tetrahedral pore volume and that of the molecule taken from reference [16].

	Molar enthalpy of immersion $-\Delta H_{imm}$ (kJ/mol)			Ratio volume (small pore/adsorbate)	
	UiO-66	HKUST-1	ZIF-8	UiO66	HKUST-1
n-hx	20.9 kJ/mol	30.7 kJ/mol	15.2 kJ/mol	2.96	1.35
2-MP	27.9 kJ/mol	35.5 kJ/mol	16.9 kJ/mol	1.39	1.12
2,2-DMB	41.4 kJ/mol	35.4 kJ/mol	0.0 kJ/mol	1.34	1.01

Simulated adsorption isotherms showed very good agreement between the saturation loading for 2-MP and n-hex but overpredicted 2,2-DMB adsorption by 1 mmol/g (Figure S6). This led us to the conclusion that 2,2-DMB may not fit inside the tetrahedral pores of HKUST-1. To further investigate the accessibility of 2,2-DMB to these pores, we repeated the simulations by denying C_6 isomers access to small tetrahedral pores. To do this, we "geometrically" blocked these pores in the simulations by not allowing any Monte Carlo moves in pre-defined region. Interestingly, the resulting isotherm (Figure S7) after pore blocking accurately predict the saturation loading of 2,2-DMB but not of n-hex or 2-MP – further proof that 2,2-DMB is too bulky to access HKUST-1's small tetrahedral pores. As shown in Figure S8, the combination of blocked tetrahedral pores for 2,2-DMB and open pores for the other isomers perfectly fit the experimental isotherms.

Moving forward to our last sample, UiO-66, the total amount adsorbed at relative pressures close to condensation is rather similar for all three hydrocarbons with uptakes around 2.9-3.0

mmol/g. However, significant differences exist between the amount of hydrocarbons adsorbed at low relative pressures. In the region between 10^{-3}-10^{-2} p/p_0, 2,2-DMB exhibits an enhanced adsorption (concave knee), followed by 2-MP with a linear profile and finally n-hx with a certain delay in the micropore filling threshold pressure. Taking into account that all three molecules are adsorbed to the same extent, one would expect that either the enthalpy per weight (J/g) or the molar enthalpy (kJ/mol) are able to predict the adsorption behavior. A closer look to Tables 2 and S4 confirms this assumption. Immersion calorimetry measurements into 2,2-DMB exhibit a large enthalpy value (119 J/g) and a larger molar enthalpy (41 kJ/mol), followed by 2-MP (80 J/g; 28 kJ/mol) and n-hx (64 J/g; 21 kJ/mol), in perfect agreement with the vapour adsorption performance at low coverages. Previous theoretical calculations described in the literature have indicated preferential adsorption of di-branched hydrocarbons in UiO-66, versus mono-branched and linear hydrocarbons.[14,31] The reverse hierarchy in UiO-66 has been recently confirmed using equimolecular breakthrough curves experiments and chromatography.[15, 16, 31] Our GCMC simulations (Figure S10) also confirmed the experimentally observed reverse hierarchy of adsorption (2,2-DMB > 2-MP > n-hx); however, they predict the saturation loading of around 2.0 mmol/g which is ca. 30% less than the experimental values for all isomers. Simulation snapshots at

low pressure (1 Pa) revealed that 2,2-DMB and 2-MP fill the small cavities as well as the large cavities in UiO-66 whereas n-hx only adsorbs in the large cavities at low pressure regime (Figure S11). At higher pressures, n-hex eventually fills the smaller pores and at saturation loading (Figure S12) 1 molecule of each hexane isomer resides in either small or large cavities of UiO-66 – suggesting that higher saturation loading measured in experiments is due to the presence of defects and hence larger pores in the experimental sample. We note that the presence of defects is also evident from the experimental N_2 adsorption isotherm not exhibiting a distinct plateau (see Figure S2).

Despite ZIF-8 with small cavities where strong confinement and size exclusion effect are observed, the reverse selectivity in MOFs can only be explained due to the interplay between specific confinement effects raising from the level of match between the pore and the adsorbate shape and size. Monte Carlo simulations performed by Dubbeldam et al. predicted inverse hierarchy only for pores around 0.6-0.7 nm, where branched hydrocarbons fit more snugly and exhibit stronger interactions with the multiple walls, while larger cavities must exhibit normal hierarchy.[14] This is for instance the case for the 3D cubic pore systems in UiO-66 and HKUST-1, consisting of octahedral and tetrahedral pores (although with different shape and size) connected by triangular windows.

The tetrahedral pores are considered the most energetically favorable adsorption sites. Recent results from Ramsahye et al. have confirmed that the degree of confinement of 2,2-DMB is larger in the tetrahedral cavities of UiO-66 and HKUST-1 (lower ratio of tetrahedral pore volume to the molecular volume - see for instance Table 2), followed by 2-MP and finally n-hx.[16] Although the order of confinement in tetrahedral cavities (2,2-DMB>2-MP>n-hx) is in close agreement with our vapour adsorption data, our calculations perfectly fit for UiO-66 but do not allow to explain the larger affinity of HKUST-1 for di-branched hydrocarbons following this hypothesis since tetrahedral cavities are inaccessible to 2,2-DMB. Rather the presence of stronger interactions with the open metal sites must account for the observed behavior in HKUST-1.

Last but not least, previous GCMC simulations only predict this selectivity order (2,2-DMB>2-MP>n-hx) for UiO-66 but not for HKUST-1. According to Ramsahye et al., GCMC simulations predict a normal selectivity (n-hx>2-MP>2,2-DMB) for HKUST-1 due to the presence of "open" tetrahedral pores in HKUST-1 that allow n-hx to be adsorbed preferentially over the branched isomers.[16] However, this is not the case in our vapor isotherms and calorimetric data. In our case, both techniques predict inverse hierarchy for UiO-66 and HKUST-1.

4. CONCLUSIONS

Here, we introduced liquid-phase immersion calorimetry as a fast and powerful technique to enable reverse hierarchy analyses for the adsorption of liquids with different size, shape and chemistry in three different MOFs: ZIF-8, HKUST-1 and UiO-66. Vapour adsorption measurements at 298 K confirmed preferential adsorption of the di-branched C_6 isomer versus n-hx and 2-MP at low pressures in UiO-66 and HKUST-1, in agreement with the calorimetry measurements. Using molecular-level simulations, we showed that this behavior is due to the preferential adsorption of 2,2-DMB in the small tetrahedral cavities, in the case of UiO-66, and the presence of strong interactions with the open metal sites, in the case of HKUST-1. Finally, we showed that whereas the enthalpy per unit gram depends on i) the number of molecules adsorbed and ii) the framework-adsorbate interactions, the molar enthalpy (kJ/mol) largely depends on the liquid-framework interactions, thus defining the adsorption performance of the MOFs at low relative pressures. These results open the gate towards the application of immersion calorimetry for the pre-screening of MOFs to identify in an easy, fast and reliable way interesting characteristics and/or properties such as separation ability, reversed hierarchy, pore

window size, presence of unsaturated metal sites, molecular accessibility, and so on.

ASSOCIATED CONTENT

Supporting Information.

Physicochemical characterization of the evaluated MOFs (XRD and gas adsorption isotherms (N_2 and Ar), Monte Carlo simulation details and comparison of experimental and predicted isotherms for n-hx, 2-MP and 2,2-DMB for UiO-66, HKUST-1 and ZIF-8 can be found in the Supporting Information.

AUTHOR INFORMATION

Corresponding Author

*Joaquín Silvestre-Albero; Email: joaquin.silvestre@ua.es

ORCID

Manuel Martínez-Escandell: 0000-0002-8995-0998

David Fairen-Jimenez: 0000-0002-5013-1194

Joaquin Silvestre-Albero: 0000-0002-0303-0817

Peyman Z. Moghadam: 0000-0002-1592-0139

Notes

Any additional relevant notes should be placed here.

ACKNOWLEDGMENT

Authors would like to acknowledge financial support from MINECO (MAT2016-80285-p), Generalitat Valenciana (PROMETEOII/2014/004) and H2020 (MSCA-RISE-2016/NanoMed Project). P.Z.M. is grateful for start-up funds from the University of Sheffield.

REFERENCES

(1) Maesen, T.; Harris, T. Process for producing high RON gasoline using CFI zeolite, in, US7037422 B2, USA, 2006.

(2) Gehre, M.; Guo, Z.; Rothenberg, G.; Tanase, S. Sustainable separations of C_4-hydrocarbons by using microporous materials. *ChemSusChem* 2017, *10*, 3947-3963.

(3) Silvestre-Albero, J.; Gómez de Salazar, C.; Sepúlveda-Escribano, A.; Rodríguez-Reinoso, F. Characterization of microporous solids by immersion calorimetry. *Colloids and Surfaces A: Phys. & Eng. Aspects* **2001**, *187-188*, 151-165.

(4) Laredo, G.C.; Trejo-Zarrada, F.; Jimenez-Cruz, F.; García-Gutierrez, J.L. Separation of linear and branched paraffins by adsorption processes for gasoline octane number improvement. Recent Patents on Chem. Eng. **2012**, *5*, 153-173.

(5) Denayer, J.F.M.; Ocakoglu, A.R.; Arik, I.C.; Kirschhock, C.E.A.; Martens, J.A.; Baron, G.V. Rotational entropy driven separation of alkane/isoalkane mixtures in zeolite cages. *Angew. Chem. Int. Ed.* **2005**, *44*, 400-403.

(6) Santilli, D.S.; Harris, T.V.; Zones, S.I. Inverse shape selectivity in molecular sieves: Observations, modelling, and predictions. *Microp. Mater.* 1993, *1*, 329-341.

(7) Denayer, J.F.M.; Ocakoglu, A.R.; Martens, J.A.; Baron, G.V. Investigation of inverse shape selectivity in alkane adsorption on SAPO-5 zeolite using a tracer chromatography technique. *J. Catal.* **2004**, *226*, 240-244.

(8) Kaskel, S. The chemistry of metal-organic frameworks, Wiley-VCH, Weinheim, Germany, 2016.

(9) Tian, T.; Zeng, Z.; Vulpe, D.; Casco, M.E.; Divitini, G.; Midgley, P.A.; Silvestre-Albero, J.; Tan, J.-C.; Moghadam, P.Z.; Fairen-Jimenez, D. A sol-gel monolithic metal-organic framework with enhanced methane uptake. *Nature Materials* **2018**, *17*, 174-180.

(10) Zhu, L.; Liu, X.-Q.; Jiang, H.-L.; Sun, L.B. Metal-organic frameworks for heterogeneous basic catalysis. Chem. Rev. **2017**, *117*, 8129-8176.

(11) Kreno, L.E.; Leong, K.; Farha, O.K.; Allendorf, M.; Van Duyne, R.P.; Hupp, J.T. Metal-organic framework materials as chemical sensors. *Chem. Rev.* **2012**, *112*, 1105-1125.

(12) Goesten, M.G.; Kapteijn, F.; Gascon, J. Fascinating chemistry or frustrating unpredictability: observations in crystal enginnering of metal-organic frameworks. *CrystEngComm* **2013**, *15*, 9249-9257.

(13) Moghadam, P.Z.; Li, A.; Wiggin, S.B.; Tao, A.; Maloney, A.G.P.; Wood, P.A.; Ward, S.C.; Fairen-Jimenez, D. Development of a Cambridge Structural Database subset: A collection of metal-organic frameworks for past, present, and future. *Chem. Mater.* **2017**, *29*, 2618-2625.

(14) Dubbeldam, D.; Krishna, R.; Calero, S.; Yazaydin, A.O. Computer-assisted screening of ordered crystalline nanoporous adsorbents for separation of alkane isomers. *Angew. Chemie Int. Ed.* **2012**, *51*, 11867-11871.

(15) Bárcia, P.S.; Guimaraes, D.; Mendes, P.A.P.; Silva, J.A.C.; Guillerm, V.; Chevreau, H.; Serre, C.; Rodrigues, A.E. Reverse shape selectivity in the adsorption of hexane and xylene isomers in MOF UiO-66. *Microp. Mesop. Mater.* 2011, *139*, 67-73.

(16) Ramsahye, N.A.; Trens, P.; Shepherd, C.; Gonzalez, P.; Trung, T.K.; Ragon, F.; Serre, C. The effect of pore shape on

hydrocarbon selectivity on UiO-66 (Zr), HKUST-1 and MIL-125(Ti) metal organic frameworks: Insights from molecular simulations and chromatography. *Microp. Mesop. Mater.* **2014**, *189*, 222-231.

(17) Dubbeldam, D.; Calero, S.; Ellis, D.E.; Snurr, R.Q. RASPA: molecular simulation software for adsorption and diffusion in flexible nanoporous materials. *Molecular Simulation* **2016**, *42*, 81-101

(18) Mayo, S.L.; Olafson, B.D.; Goddard, W.A. DREIDING: a generic force field for molecular simulations. *J. Phys. Chem.* **1990**, *94*, 8897–8909.

(19) Rappe, A.K.; Casewit, C.J.; Colwell, K.S.; Goddard III, W.A.; Skiff, W.M. UFF, a full periodic table force field for molecular mechanisms and molecular dynamics simulations. *J. Am. Chem. Soc.* **1992**, *114*, 10024–10035.

(20) Martin, M.G.; Siepmann, J.I. Novel configurational-bias Monte Carlo method for branched molecules: Transferable potentials for phase equilibria.2. United-atom description of branched alkanes. *J. Phys. Chem. B* **1999**, *103*, 4508–4517.

(21) Moellmer, J.; Celer, E.B.; Luebke, R.; Cairns, A.J.; Staudt, R.; Eddaoudi, M.; Thommes, M. Insight on adsorption characterization of metal-organic frameworks: A benchmark study on the novel *soc*-MOF. *Microp. Mesop. Mater.* **2010**, *129*, 345-353.

(22) Silvestre-Albero, J.; Silvestre-Albero, A.; Rodríguez-Reinoso, F.; Thommes, M. Physical characterization of activated

carbons with narrow microporosity by nitrogen (77.4 K), carbon dioxide (273 K) and argon (87.3 K) adsorption in combination with immersion calorimetry. *Carbon* **2012**, *50*, 3128-3133.

(23) Cuadrado-Collados, C.; Fernández-Catalá, J.; Fauth, F.; Cheng, Y.Q.; Daemen, L.L.; Ramirez-Cuesta, A.J.; Silvestre-Albero, J. Understanding the breathing phenomena in nano-ZIF-7 upon gas adsorption. *J. Mater. Chem. A.* **2017**, *5*, 20938-20946.

(24) Gutierrez, I.; Diaz, E.; Vega, A.; Ordoñez, S.; Guerrero-Ruiz, A.; Castillejos-Lopez, E.; Rodriguez-Ramos, I. Hydrocarbons adsorption on metal trimesate MOFs: Inverse gas chromatography and immersion calorimetry studies. *Thermochimia Acta* **2015**, *602*, 36-42.

(25) Huang, X.-C.; Lin, Y.-Y.; Zhang, J.-P.; Chen, X.-M. Ligand-directed strategy for zeolite-type metal-organic frameworks: zinc(II) imidazolates with unusual zeolitic topologies. *Angew. Chemie Int. Ed.* **2006**, *45*, 1557-1559.

(26) Fairén-Jimenez, D.; Galvelis, R.; Torrisi, A.; Gellan, A.D.; Wharmby, M.T.; Wright, P.A.; Mellot-Draznieks, C.; Düren, T. Flexibility and swing effect on the adsorption of energy-realted gases on ZIF-8: combined experimental and simulation study. *Dalton Transactions* **2012**, *41*, 10752-10762.

(27) Hobday, C.L.; Woodall, C.H.; Lennox, M.J.; Frost, M.; Kamenev, K.; Düren, T.; Morrison, C.A.; Moggach, S.A. Understanding the adsorption process in ZIF-8 using high pressure crystallography and computational modelling. *Nature Commun.* **2018**, *9*, 1429.

(28) Hulvey, Z.; Lawler, K.V.; Qiao, Z.; Zhou, J.; Fairen-Jimenez, D.; Snurr, R.Q.; Ushakov, S.V.; Navrotsky, A.; Brown, C.M.; Foster, P.M. Noble gas adsorption in copper trimesate, HKUST-1: An experimental and computational study. *J. Phys. Chem. C* **2013**, *117*, 20116-20126.

(29) Valenzano, L.; Civalleri, B.; Chavan, S.; Bordiga, S.; Nilsen, M.H.; Jakobsen, S.; Lillerud, K.P.; Lamberti, C. Disclosing the complex structure of UiO-66 metal organic framework: A synergic combination of experiment and theory. *Chem. Mater.* **2011**, *23*, 1700-1718.

(30) Farruseng, D.; Daniel, C.; Gaudillère, C.; Ravon, U.; Schuurman, Y.; Mirodatos, C.; Dubbeldam, D.; Frost, H.; Snurr, R.Q. Heats of adsorption for seven gases in three metal-organic frameworks: Systematic comparison of experiment and simulation. *Langmuir* **2009**, *25*, 7383-7388.

(31) Duerinck, T.; Bueno-Perez, R.; Vermoortele, F.; De Vos, D.E.; Calero, S.; Baron, G.V.; Denayer, J.F.M. Understanding

hydrocarbon adsorption in the UiO-66 metal-organic framework: Separation of (un)saturated linear, branched, cyclic adsorbates, including stereoisomers. *J. Phys. Chem. C* **2013**, *117*, 12567-12578.

TOC Graphic